

# Power Losses in Enlarged Experimental Chambers of the LHC

L. Vos SL/AP

Keywords : impedance, electromagnetic fields, higher order modes, interaction region

---

## Summary

Expressions for resonant frequencies and shunt impedances are derived for enlarged interaction region vacuum pipes of the type proposed in CMS. They are used to compute the power that the multi-bunch LHC beams can dissipate in such a structure if one of its resonant frequencies is equal to a harmonic of the beam intensity. This power can be several kilowatts for a specific rigid geometry. It is demonstrated that the actual power dissipation in a resonance is reduced to only a few watts for beam pipes that are not thermally constrained. The maximum local temperature increase is at most  $45^\circ K$ , which can be considered to be acceptable.

---

## 1 Introduction

The aim of this work is to estimate the power deposited by LHC beams in an enlarged vacuum chamber. Interaction region vacuum chambers often belong to this category. The basic structure that is studied is illustrated in Figure 1.

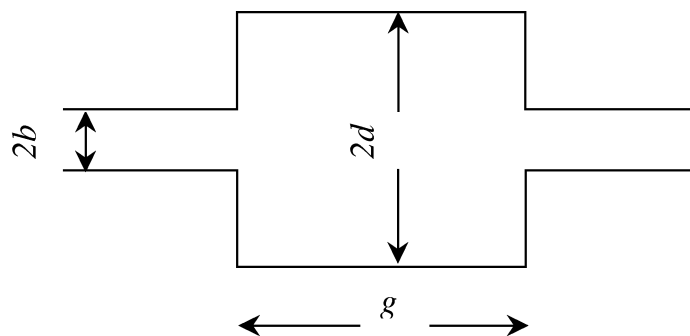


Figure 1 : Basic geometry

The maximum frequency considered is the cut-off frequency of the connecting pipe with radius  $b$ . At higher frequencies the power is carried away in the pipe. The propagation constant in the enlarged vacuum chamber with radius  $d$  is :

$$\gamma = \sqrt{\left(\frac{\tau_0}{d}\right)^2 - \left(\frac{\omega}{c}\right)^2} . \quad (1)$$

The lowest cut-off frequency of the pill box is  $\omega_{co} = c\tau_0/d$ , where  $\tau_0 = 2.4$  the first root of Bessel function  $J_0$ .

## 2 Low frequency regime

In this regime  $\omega$  is smaller than  $\omega_{co}$ . The inductance of the structure is given by [1]:

$$L(\omega) = \frac{\mu_0}{2\pi} \ln\left(\frac{d}{b}\right) \frac{1 - e^{-\gamma(\omega)g}}{\gamma(\omega)} . \quad (2)$$

The propagation constant  $\gamma$  is real. For very low frequencies it is large so that:

$$L = \frac{\mu_0}{2\pi} \frac{d}{\tau_0} \ln\left(\frac{d}{b}\right) . \quad (3)$$

At the other extreme in this frequency regime,  $\omega$  approaches  $\omega_{co}$  and  $\gamma(\omega)g$  becomes very small such that:

$$L(\omega \rightarrow \omega_{co}) = \frac{\mu_0}{2\pi} \ln\left(\frac{d}{b}\right) g . \quad (4)$$

$$Z = j\omega L$$

The effect of a sloping edge or taper (see Fig 2) is included as a function of its angle  $\theta$ .

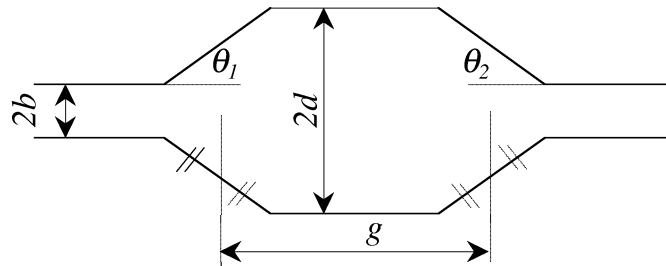


Figure 2 : Pill box with edges sloping with angles  $\theta_1$  (left) and  $\theta_2$  (right)

The impedance is lowered proportional to the *sine* of sloping angles since the reflected fields are being redirected according to [2]:

$$Z_\theta = Z \frac{\sin(\theta_1) + \sin(\theta_2)}{2} . \quad (5)$$

The impedance is purely imaginary and no power dissipation takes place.

### 3 High frequency regime

Consider now frequencies above cut-off of the pill box, i.e.  $\omega > \omega_{co}$ , but below the cut off frequency of the connecting tube ( $\omega < c\tau_0/b$ ). The propagation constant  $\gamma$  is imaginary and many resonant modes exist. In the limit of  $b = 0$  (closed pill box cavity)[1] one finds:

$$R/Q = Z_0 \frac{g}{2d}, \quad (6)$$

where  $Z_0$  is the impedance of free space. If side tubes with radius  $b$  are attached to the pill box and  $b > d/4$  then the impedance is reduced as :

$$R/Q = \frac{Z_0}{2\pi} \frac{g\tau_0}{d} \ln \frac{d}{b}. \quad (7)$$

In this frequency regime it is necessary to introduce the transit-time factor  $T$  which takes into account the time that a charged beam particle interacts with the pill box:

$$T = \frac{\sin\left(\frac{\omega g}{2c}\right)}{\frac{\omega g}{2c}}. \quad (8)$$

As shown in [3], the impedance is multiplied by  $T^2$ . This then leads to a general formula for the  $R/Q$  of a tapered enlarged cylindrical vacuum chamber neglecting the effect of side tubes:

$$R/Q = Z_0 \frac{g}{2d} T^2 \frac{\sin(\theta_1) + \sin(\theta_2)}{2}. \quad (9)$$

Basically the impedance in this frequency regime consists of a series of lossless oscillators. Their frequencies can be computed with :

$$\omega_n = \pi c \sqrt{\left(\frac{n}{g}\right)^2 + \left(\frac{\tau_m}{\pi d}\right)^2}, \quad (10)$$

where  $\tau_0, \tau_1, \dots$  are zero's of Bessel functions and  $n=0,1,2,\dots$

It may be interesting to compute the energy that a bunch with Gaussian intensity profile ( *rms* bunch length  $\sigma_t$  ) leaves behind after a single passage in one such resonator with resonant frequency  $\omega_{res} = \omega_n$ . This energy is found by computing the convolution integral between the spectrum of the square of the bunch intensity (1 C charge is assumed) and the impedance of the oscillator. The result of this computation is commonly known as the longitudinal loss factor  $k_{ll}$ .

$$k_{ll} = \frac{1}{2\pi} \int Z(\omega) I^2(\omega) d\omega = \frac{\omega_{res} (R/Q)}{2} e^{-(\omega_{res} \sigma_t)^2}. \quad (11)$$

The energy is not dissipated in this particular case. It only makes the resonator ring forever.

The spectrum of a single bunch that passes only once is a continuum and the overlap integral of this continuous spectrum and the resonant curve is finite (Eq 11). The spectrum of a bunched beam circulating in a machine is a line spectrum. If one of these lines, which are infinitely narrow, coincides exactly with a resonant mode, then the corresponding loss factor would go to infinity since the shunt impedance of a lossless resonator is infinite and its quality factor  $Q$  is infinite as well.

It is obvious that practical pill box structures do not have infinitely large quality factors. In this context it is worth to mention that the  $Q$ 's of the LEP SC cavities exceed  $10^9$  ! The finite conductivity of the pill box introduces losses and lowers both the shunt impedance and the quality factor. The definition of the quality factor  $Q$  is:

$$Q = 2\pi \frac{W_{stored}/cycle}{W_{lost}/cycle}. \quad (12)$$

It is assumed that the average field is 1/2 of the peak field. The energy stored per cycle is then:

$$\frac{W_{stored}}{cycle} = \frac{\mu_0 \omega_{res}}{2\pi} \frac{H^2}{4} V, \quad (13)$$

where  $W$  is the energy,  $V$  is the volume of the pill box and  $H$  the peak magnetic field. The power that is lost follows from the Poynting vector penetrating into the pill box walls:

$$P_{lost} = R_s \frac{H^2}{2} A, \quad (14)$$

where  $R_s$  is the surface resistance and  $A$  the area of the pill box walls.

$$R_s = \sqrt{\frac{\omega_{res} \mu_0 \rho}{2}}, \quad (15)$$

$\rho$  is the resistivity. This then yields the quality factor :

$$Q = \sqrt{\frac{\omega_{res} \mu_0}{2\rho}} \frac{V}{A} = \frac{V}{\delta_s A} = \frac{V}{V_{loss}}, \quad (16)$$

$\delta_s$  is the skindepth and  $V_{loss}$  is the volume in which the losses are dissipated. For cylindrical structures which are not too short this simplifies to:

$$Q = \frac{d}{2\delta_s}. \quad (17)$$

With Eq. 9 this yields a value for the shunt impedance for each of the resonators:

$$R_{sh} = Z_0 \frac{g}{4\delta_s} T^2 \frac{\sin(\theta_1) + \sin(\theta_2)}{2}. \quad (18)$$

The properties of a pill-box like structure are completely determined by Equations 9,10,17 and 18. The problem of power deposition by a LHC beam will be studied in the following sections. The structure can be of any dimension but for illustrative purposes, a CMS type

conical vacuum chamber has been assumed. It is straightforward to extend the computation to other cylindrical vacuum vessels.

## 4 Power deposition in an enlarged cylindrical vacuum chamber by LHC beams

### 4.1 Spectrum of the LHC beam

The LHC beam consists of bunches with *rms* length  $\sigma_t = 0.25$  ns and bunch population  $n_b = 1.1 \cdot 10^{11}$ . The frequency spectrum of these bunches goes up to  $\omega/2\pi = 3/2\pi\sigma_t \sim 2$  GHz. The bunch separation is  $T_b = 24.95$  ns, corresponding to the basic bunching frequency  $f_B = 40$  MHz. The nominal DC beam intensity is  $I = 0.56$  A.

The bunch train is arranged in batches. The batch structure creates side bands for each 40 MHz harmonic. The batch structure contains three basic patterns.

The first pattern is imposed by the PS and consists of 72 bunches with a separation of 8 bunch spaces. It will give rise to a number of harmonics with a frequency spacing of 0.5 MHz. The next pattern is imposed by the SPS and consists of a train with a length of 232 bunch spaces and separated by 38. The harmonics have a frequency spacing of 0.15 MHz. The last pattern is imposed by the LHC itself and consists of a train with 3445 bunch spacings and a gap of 119. It generates harmonics at the revolution frequency. The total harmonic structure due to the batch modulation is shown in Fig 3. It can be seen that the LHC batch pattern hardly contributes. If the power of the basic 40 MHz harmonic is unity, then the total power of the side bands amounts to 0.15. Most of it is confined in a band of a few MHz.

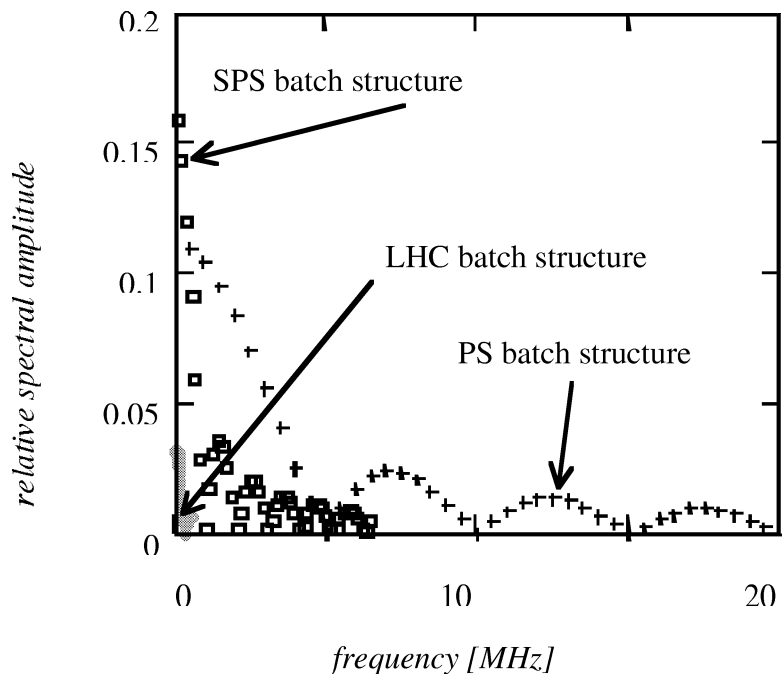


Figure 3 : Spectrum of LHC beam. The intensity of the basic 40 MHz harmonic is taken as unity.

## 4.2 Spectrum and power of pill box resonators

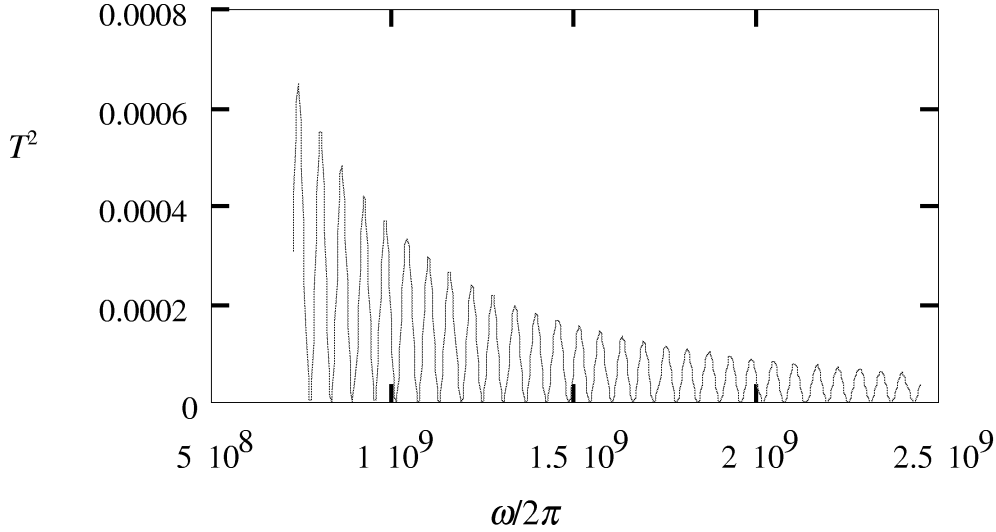


Figure 4 : Typical  $T^2$  for a chamber (CMS) with  $b = 0.047$  m,  $d = 0.158$  m,  $g = 9$  m,  $\theta_1 = 0.0149$ ,  $\theta_2 = 0.26$  (see Fig 2).

The frequencies of the resonators span from the lowest cut-off frequency of the pill box ( $c\tau_\phi/d$ ) to the cut-off frequency of the connecting beam tube ( $c\tau_\phi/b$ ). The envelope of the respective shunt impedances is determined by the transit time factor  $T^2$ . It is shown in Fig 4 for a CMS like chamber.

It is obvious that the lowest frequencies are the more important ones. A basic beam harmonic, intensity  $I$ , dissipates a power  $P_n$  in a resonator, shunt impedance  $R_{shn}$ , which has the same frequency as the harmonic :

$$P_n = 4I^2 R_{shn} = 4I^2 (R/Q)_n Q_n, \quad (19)$$

where the index  $n$  identifies the resonance and its frequency as defined by Eq. 10. The two LHC beams cross each other in the experimental chambers. Therefore the power is computed assuming two beams of nominal intensity ( $I=0.56$  A). The currents of both (identical) beams cancel at the crossing point which is infinitesimally short. The current cancellation disappears over half the bunch length ( $\sim 0.04$  m) on either side of the crossing. This effect will be ignored since it occurs over a length which is very short compared to the length of experimental chambers in the LHC.

It is convenient to call effective impedance the product of the shunt impedance and the square of the bunch spectrum. This quantity is plotted in Fig 5 for each of the structure resonances between 0.72 and 1.44 GHz. It is assumed that the inner side of the pill-box is coated with copper. The part beyond 1.5 GHz of the frequency range of the resonances has been skipped since the shunt impedance has dropped to negligible values due to the combined effect of the transit time factor and the bunch spectrum. The exact locations of the structure resonances for the chosen geometry are indicated by the vertical gridlines. The power that is generated by the beam in a resonator if one of the resonances overlaps with a beam harmonic can be found with Eq. 19. For example, a resonance with an impedance of 1000  $\Omega$  excited by a beam harmonic will dissipate 1250 W for nominal beam intensity,  $I = 0.56$  A.

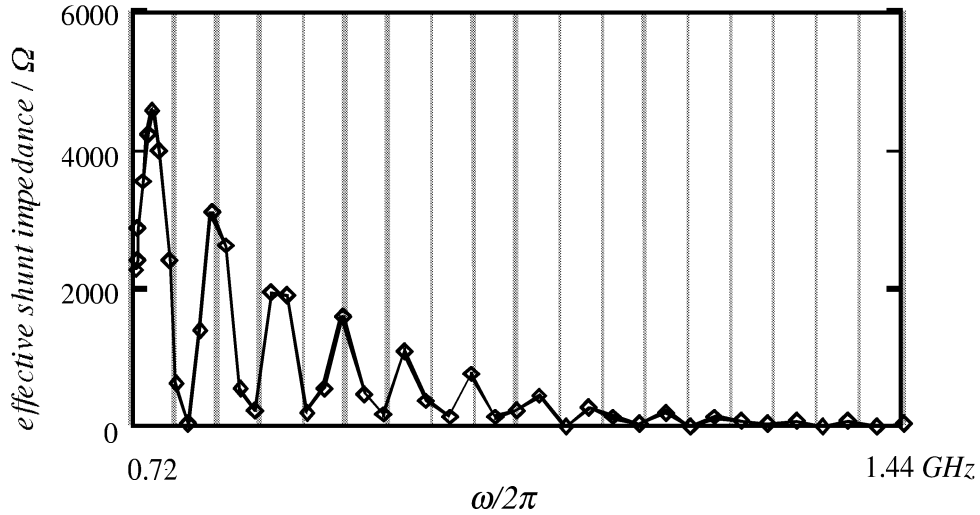


Figure 5 : Effective shunt impedance of each resonance. The chamber is a CMS type structure with copper coating on the inside. The frequencies of the 40 MHz beam harmonics are indicated by the gridlines.

### 4.3 Combination of beam spectrum and resonance spectrum

The rather large frequency range of Fig 5 makes it rather difficult to judge to what extent structure resonances and beam harmonics overlap. Their relative positions become more evident when plotting the shunt impedances of the resonances in a single frequency bin with a width of 40 MHz. The result is shown in Fig 6. Resonances located near the edge are close to a beam harmonic, those in the middle are at maximum distance (20 MHz).

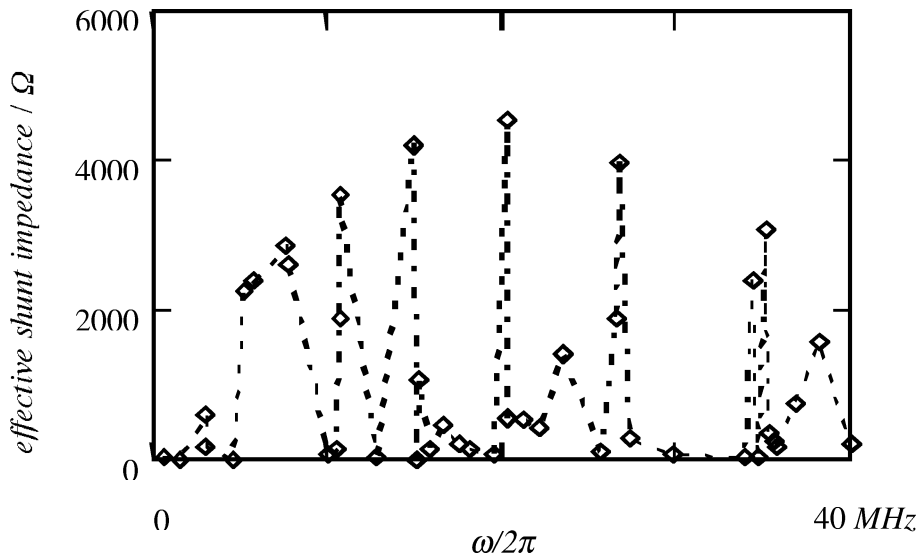


Figure 6 : Effective shunt impedance of each resonator of CMS chamber translated into a single frequency bin of 40 MHz.

While the beam spectral lines are well defined in frequency and are extremely narrow banded this is not the case for the structure resonances. Indeed, small changes in dimensions may change the location of the resonances with respect to the beam harmonics drastically. Moreover, the resonances spread over several 0.1 MHz in the case of a copper clad pill box chamber. Since the real geometry cannot be known with sufficient precision, no guarantee can

be given that resonances, with a potential power of say a few 100 W (shunt impedance a few 100  $\Omega$ ), will never cross a beam spectral line, not to mention one of its numerous batch modulation side bands (see Fig 3).

#### 4.4 *Dependence of resonant frequencies on the geometry of pill boxes*

The dependence of the resonant frequencies on the dimensions can be found by differentiation of Eq. 10:

$$\frac{d\omega_n}{\omega_n} = -\frac{\left(\frac{n}{g}\right)^2}{\left(\frac{n}{g}\right)^2 + \left(\frac{\tau}{\pi d}\right)^2} \frac{dg}{g} \approx \left(\frac{\pi n d}{\tau g}\right)^2 \frac{dg}{g}. \quad (20)$$

The resonant frequencies appear to be relatively insensitive to length variations of the vacuum chamber for the low (important) mode numbers.

$$\frac{d\omega_n}{\omega_n} = -\frac{\left(\frac{\tau}{\pi d}\right)^2}{\left(\frac{n}{g}\right)^2 + \left(\frac{\tau}{\pi d}\right)^2} \frac{d(d)}{d} \approx \frac{d(d)}{d} \quad (21)$$

The transverse dimensions are much more critical. A difference of 5/1000 in the maximum radius  $d$  of a CMS like chamber will shift the resonant frequencies by  $\sim 5$  MHz and will change completely the aspect of Fig 6.

#### 4.5 *Overlap of a beam spectral line with a resonance.*

Consider the static case first whereby the geometry is constant in time. One beam spectral intensity line overlaps exactly with a structure resonance. The power deposition can be found by multiplying the relevant shunt impedance and the factor  $4I^2 = 1.25$  for nominal LHC beam conditions (see Eq. 19). This power can be considerable as can be seen from Fig 5 and 6. The power has to be removed from the chamber by a cooling system in order to maintain its dimensions. The static case is purely academic and it is more interesting and more realistic to consider the dynamic case: an experimental vacuum chamber without forced cooling such that the dimensions of the chamber are allowed to vary to some extent.

Some amount of power will dissipate in the chamber wall whenever a beam harmonic falls within the bandwidth of a resonator. The power heats up the walls causing thermal expansion. The increase in chamber dimensions, however small, will reduce the resonant frequency. The level of power dissipation will change as will the dimensions of the chamber...The process continues until thermal (dimension and resonant frequency) and electrical (power) equilibrium are reached. This process and its equilibrium are illustrated in Fig 7.



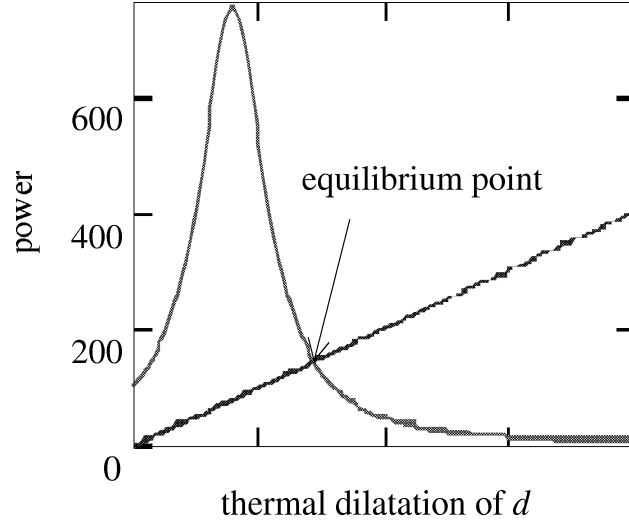


Figure 7: Dissipated power as a function of variation of the transverse dimension of the vacuum chamber (top curve) and thermal expansion as a (linear) function of the dissipated power (bottom curve). The frequency decreases towards the right hand side.

The initial conditions are at the left hand side of the plot. The beam harmonic is within the resonant curve but well below resonance in this example. Heating causes thermal expansion which shifts the resonance downwards (toward the right of the plot), further enhancing thermal dilatation. The process stops at the point of intersection where the dissipated power is just equal to the power needed to sustain the thermal expansion. This equilibrium can be found as follows. Consider a pill box resonance with resonant frequency  $\omega_n$  and quality factor  $Q_n$ . When the frequency of a beam spectral line is exactly equal to the resonant frequency then the dissipated power is  $P_n$ . When the frequency of the beam harmonic is  $\omega_b \neq \omega_n$ , then the power is  $p(\omega_n) < P_n$  :

$$p(\omega_n) = \frac{P_n}{1 + Q_n^2 \left( \frac{\omega_n - \omega_b}{\omega_b} \right)^2} = \frac{P_n}{1 + Q_n^2 \left( a - \frac{1}{a} \right)^2}. \quad (22)$$

The radius  $d$  increases by an amount  $\delta$  due to thermal dilatation and  $\omega_n$  decreases (Eq 21). Hence :

$$p(\delta) = \frac{P_n}{1 + Q_n^2 \left( a \left( 1 - \frac{\delta}{d} \right) - \frac{1}{a \left( 1 - \frac{\delta}{d} \right)} \right)^2} \approx \frac{P_n}{1 + Q_n^2 \left( a - \frac{1}{a} - \frac{\delta}{d} \left( a + \frac{1}{a} \right) \right)^2}. \quad (23)$$

The thermal expansion depends on the dissipated power :

$$\delta = \alpha_\theta d R_\theta p, \quad (24)$$

$\alpha_\theta$  is the thermal expansion coefficient and  $R_\theta$  is the thermal resistance of the vacuum

chamber. If the bulk of the chamber is stainless steel then  $\alpha_\theta = 19.1 \cdot 10^{-6}/K$ . The thermal resistance can be found with :

$$R_\theta = \frac{1}{4\varepsilon_\theta\sigma_\theta T^3 2\pi dl}, \quad (25)$$

$\varepsilon_\theta = 0.08$  is the emissivity of stainless steel,  $\sigma_\theta = 5.67 \cdot 10^{-8} W/m^2 K^4$  is Boltzmann's constant,  $T = 300^\circ K$  is the ambient temperature and  $l$  is the length of the radiating part of the chamber. The equilibrium condition can be found by equating Eq 23 and Eq 24. The extreme values for the power and the temperature rise depend on the initial conditions. The upper limits are:

$$P_{equi} \leq 2 \frac{P_n^{1/3}}{(2Q_n \alpha_\theta R_\theta)^{2/3}}; \quad \Delta T_{equi} \leq 2 \frac{(R_\theta P_n)^{1/3}}{(2Q_n \alpha_\theta)^{2/3}}. \quad (26)$$

Using Eq 19 finally yields :

$$P_{equi} \leq \frac{2}{Q_n^{1/3}} \left( \frac{I^2 (R/Q)_n}{\alpha_\theta^2 R_\theta^2} \right)^{1/3}; \quad \Delta T_{equi} \leq \frac{2}{Q_n^{1/3}} \left( \frac{R_\theta I^2 (R/Q)_n}{\alpha_\theta^2} \right)^{1/3}. \quad (27)$$

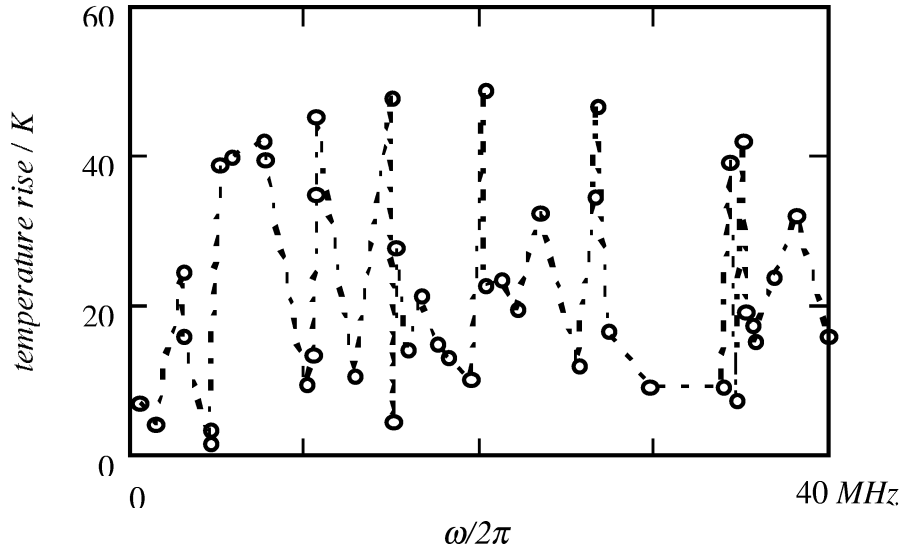


Figure 8: Maximum temperature rise associated with resonant frequencies in CMS chamber

It is important to observe that the equilibrium power and temperature rise are both inversely proportional to the cubic root of the quality factor of the resonator. Therefore it is not useful to add damping resistors. It turns out that the power in copper clad chambers is about half the power dissipated in chambers in naked stainless steel. It is therefore prudent to prescribe copper coating. It is interesting to note that the temperature rise is only a weak function of the radiating length  $l$ . This length is roughly defined by that part of the tapered chamber where the resonant frequency is above the cut-off. For conical chambers like the CMS one this amounts to only a few % of the total length for low mode numbers. Fig 8 shows a plot of the maximum temperature rise associated with each resonance in a CMS like chamber and Fig 9 shows the corresponding effective shunt impedance in the equilibrium state. The resonances and the frequency scale are the same as in Fig 6.

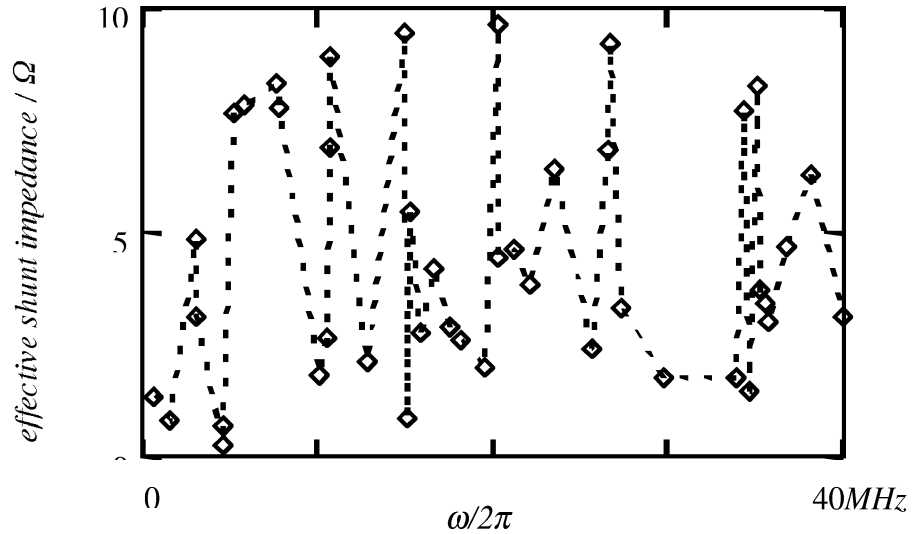


Figure 9: Effective shunt impedance of resonances in CMS chamber in thermal equilibrium

The maximum effective shunt impedance of the resonances has dropped by a factor 500 from  $\sim 5 \text{ k}\Omega$  to  $\sim 10 \text{ }\Omega$  between the situation of Fig 6 (static case) and Fig 9 (dynamic case).

A last feature to be pointed out is the effective bandwidth of the resonances. It is clear that the thermo-electric loop is not active when the exciting  $40 \text{ MHz}$  harmonic is too far away from the resonant frequency. However it turns out that the loop has an effective bandwidth which is 20-30 times larger than the *rms* bandwidth of the resonance. Consequently there is a 50% chance that one beam harmonic falls within the effective bandwidth of a structure resonance. Nevertheless, this is not a real problem since the power levels are so low.

The estimation of power and temperature rise are based on the effect of the  $40 \text{ MHz}$  harmonics alone. It is justified to query about the contribution of the batch modulation harmonics. Several beam spectral components are now involved simultaneously in the initial conditions. Each resonance can be included by simple addition in a plot like Fig 7 and the same procedure can be applied. The peak spectral power of the batch modulation harmonics is two orders of magnitude smaller than the peak spectral power of the main harmonics (Fig 3). They will increase considerably the number of low power resonators (see Fig 5 and 6). The probability becomes very high that a beam harmonic (fundamental or batch pattern harmonic) couples with a structure resonance. However, the power generated by the batch pattern harmonics will be less than  $1 \text{ W}$  and is accompanied by a temperature rise of a few  $K$  at most.

## 5 Conclusion

The power that may be generated by the nominal LHC beams in one of the many possible resonances of an enlarged experimental vacuum chamber can be in the order of  $kW$ 's if a fundamental beam harmonic happens to have the same frequency as one of the many possible resonances of the structure. The probability of such an event is relatively low but it cannot be totally excluded for a chamber with parameters that are stable in time and independent of power dissipation. However, if the vacuum chamber is not thermally constrained such that its dimensions can change freely, then a thermo-electrical equilibrium state exists whereby the maximum power deposition is at most a few *watts* and the concomitant maximum temperature rise less than  $45 \text{ }^\circ K$ . Therefore, the influence of the LHC beam on a CMS-like experimental chamber is operationally acceptable. It is not recommended to damp the resonances with resistors nor to remove the internal copper coating

of a stainless steel structure since the expected potential power dissipation and the steady state temperature rise will be higher in that case. A copper layer thickness of a few skin depths ( $<10 \mu m$ ) at the lowest resonant frequency is sufficient for this purpose.

## **Acknowledgements**

I am grateful to Yun Luo for the numerical verifications that he performed with the computer program MAFIA and to D. Brandt for his comments and suggestions.

## **References**

- [1] L. Vos, *Calculations and Simulations concerning the Longitudinal Impedance of an Accelerator Vacuum Chamber*, SPS/DI-MST/Note/84-2, 1984.
- [2] K. Yokoya, *Impedance of slowly tapered Structures*, CERN/SL/90-88 (AP), 1990.
- [3] G. Lambertson, *Electromagnetic Detectors*, LBL, January 1989.